Available online at www.sciencedirect.com
ScienceDirect
Sensors and Actuators B 122 (2007) 7–13
SENSORS AND ACTUATORS B CHEMICAL
www.elsevier.com/locate/snb

Carbon nanofiber/polypyrrole nanocable as toxic gas sensor

Jyongsik Jang *, Joonwon Bae

Hyperstructured Organic Materials Research Center, School of Chemical and Biological Engineering, Seoul National University, Shinlimdong 56-1, Seoul 151-742, Korea

Received 30 December 2005; received in revised form 2 May 2006; accepted 2 May 2006
Available online 27 June 2006

Abstract

Carbon nanofiber (CNF)/polypyrrole (PPy) coaxial nanocables were successfully fabricated via one-step vapor deposition polymerization (VDP), and their capability to perceive irritant gases such as ammonia (NH_3) and hydrochloric acid (HCl) was systematically examined. The Fourier transform infrared (FT-IR) spectra confirmed the formation of a PPy layer on the CNF surface. In addition, a transmission electron microscopy (TEM) image represented the formation of an ultrathin and uniform PPy layer onto the surface of CNF. The thickness of the PPy layer was conveniently controlled by varying the feeding amount of the corresponding monomer. The PPy-coated CNF exhibited an enhanced response signal due to the presence of the thin and uniform conducting polymer layer, and their response was strongly dependent on the thickness of the PPy layer.

Keywords: Vapor deposition polymerization; Carbon nanofiber; Polypyrrole; Coaxial nanocable; Sensor; Toxic gas

1. Introduction

Among various carbon nanostructures, carbon nanofibers (CNFs) have recently attracted a great interest in diverse application areas owing to their unique characteristics such as excellent chemical/mechanical stability and possibility of mass production [1–3]. Especially, CNFs are promising candidate materials for hydrogen storage devices [4], electronic components [5], catalysts and catalytic supports [6], bioanalytical tools [7], functional nanocomposites [8], field emission devices [9], and substitutes for carbon nanotubes (CNTs) [10]. Such a recent outburst of CNF-based study may originate from their chemical similarity to fullerenes and CNTs. Moreover, CNFs are distinctive high-surface-area materials that can expose exclusively either basal graphite planes or edge planes. Despite of these advantages, a little research has been so far done on the development of CNF-based sensors due to their inherent chemical and environmental stability [11].

Conducting polymers such as polypyrrole (PPy), polyaniline, and polythiophene have exhibited beneficial properties attributed to their characteristic π-electron conjugation system [12,13]. In particular, the oxidation level of conducting polymers can be easily tuned by the doping/dedoping (oxidation/reduction) mechanism. Thus, conducting polymers are sensitive to specific chemical/biological species, and they are also capable of showing an improved performance as chemical sensors [14]. As a typical example, PPy has been extensively utilized as a sensing element to recognize various analytes. PPy can be easily synthesized and possesses its inherent advantages such as a low band gap, tunable electrical conductivity, environmental stability and electrochromic properties [15,16]. PPy is capable of presenting noticeable responses to different types of chemical vapors, including acids, bases, alcohols, and alkanes via distinctive response mechanisms [17–22].

When CNF is combined with PPy, the CNF/PPy coaxial nanocables may provide an enhanced performance with mechanical durability and improved electrical conductivity. Furthermore, the ultrathin and uniform deposition of a PPy layer (<100 nm) onto the CNF surface can furnish excellent environmental stability, tunable surface property, and enhanced sensitivity. Accordingly, the resulting CNF/PPy coaxial nanocables are expected to exhibit an improved sensor performance compared with single pristine CNF or PPy.

From the viewpoint of uniform and ultrathin polymer coating, vapor deposition polymerization (VDP) provides the polymerization step of vaporized monomers under a vacuum condition

* Corresponding author. Tel.: +82 2 880 7069; fax: +82 2 888 1604.
E-mail address: jsjang@plaza.snu.ac.kr (J. Jang).

0925-4005/$ – see front matter © 2006 Elsevier B.V. All rights reserved.
doi:10.1016/j.snb.2006.05.002

and forms the polymer ultrathin layer onto the curved CNF surface. This VDP method may be applicable to surface modification, promotion of adhesion to substrate, and coating of polymeric materials on complicated geometries [23,24]. Until now, a considerable effort has been devoted toward efficient detection of irritant and toxic gases such as ammonia (NH_3), hydrochloric acid (HCl) and NO_x for human health and environment protection [25–29]. Representatively, PPy has been widely exploited as an NH_3 sensor [28–30]. In contrast, detection of HCl has been mainly achieved by polyaniline or its derivatives, because these materials are readily doped with HCl [31–33]. Meanwhile, CNT/polymer hybrids have been utilized for detection of both NH_3 and HCl [33–37]. However, incorporation of CNF-based materials into a toxic gas sensor has not yet been explored. Accordingly, the motivation of this study is to deposit a uniform and ultrathin PPy layer onto the CNF surface by a one-step VDP method and to investigate the feasibility of CNF/PPy coaxial nanocables as a highly sensitive sensor. This work is a first experimental demonstration for realization of an efficient toxic gas sensor based on the CNF/conducting polymer hybrid. In addition, the chemical response of CNFs encapsulated with PPy was also evaluated with variation in thickness of the PPy layer.

2. Experimental

2.1. Materials

CNFs with an average diameter of 50 nm were synthesized according to a well-established method, as described in the next section. Fig. 1 exhibits the scanning electron microscope (SEM) image of the CNFs employed in this work. The detailed preparation conditions and physical properties of the CNF were summarized in Table 1. Pyrrole (Py) monomer was purchased from Aldrich (Milwaukee, WI, USA) and used without further purification [38,39]. Iron(III) chloride as a redox initiator was also purchased from Aldrich and employed as received.

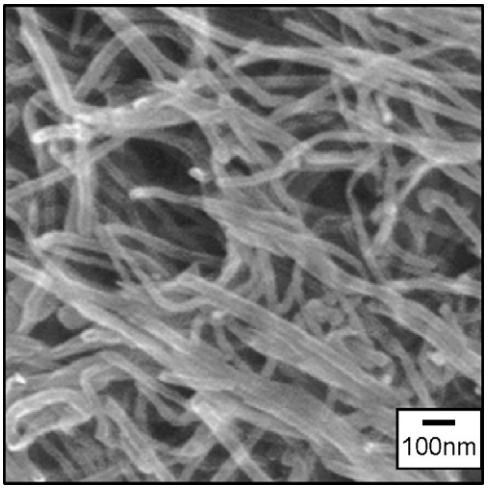

Fig. 1. SEM image of CNFs with an average diameter of 50 nm prepared from a mixed gas of carbon monoxide/ethylene and hydrogen ($CO/C_2H_2/H_2 = 2/2/1$ (v/v/v)) on a non-supported iron catalyst at 600 °C.

Table 1
Preparation conditions and physical properties of CNF

Preparation conditions	
Catalyst	Fe
Temperature (°C)	600
Reaction time (h)	1
Gas composition ($CO/C_2H_2/H_2$) (v/v/v)	2/2/1
Physical properties	
Structure	Platelet
Average diameter (nm)	80
H/C (Atomic ratio)	0.035
D_{002} (XRD) (nm)	0.3363
Surface area (m^2/g)	134

2.2. Synthesis of CNFs

CNFs were prepared from a mixed gas of carbon monoxide, ethylene and hydrogen ($CO/C_2H_2/H_2 = 2/2/1$, v/v/v) on a non-supported iron catalyst at 600 °C using a conventional horizontal tube furnace [2]. The iron catalyst powder used was prepared via precipitation of ferric carbonate by adding ammonium bicarbonate, as described by Best and Russell [40]. The precipitate was dried overnight in an oven at 100 °C and then calcined in air at 400 °C for 5 h to convert the carbonate into oxide. The calcined oxide was reduced in a 10% H_2/He mixture for 20 h at 480 °C. The reduced catalyst was subsequently cooled to ambient temperature in a helium atmosphere before being passivated in a 5% Air/He mixture for 1 h at room temperature. The passivated catalyst was then removed from the reactor and stored for later use. A quartz flow reactor for the preparation of CNFs was heated in a conventional horizontal tube furnace. The gas flow to the reactor was precisely monitored and regulated with MKS mass flow controllers. The powdered catalyst (30 mg) was placed in a quartz boat at the center of the reactor tube in the furnace. After reduction in a 10% H_2/He mixture for 2 h at the prescribed temperature, helium was flushed for 0.5 h. The reactant gas mixture of $CO/C_2H_2/H_2$ (2/2/1, v/v/v) was then allowed to flow over the catalyst for 1 h. The total amount of carbon deposited for 1 h on stream was determined gravimetrically after the system was cooled to ambient temperature. The prepared carbon was partially oxidized at 450 °C for 30 min under an air flow (100 mL/min) using the same type of horizontal furnace to remove amorphous carbons on the CNF surface. Hydrogen (99.999%), carbon monoxide (99.9%) and He (99.99%) were obtained from MG industries and used without further purification. Reagent grade iron nitrate ($Fe(NO_3)_3 \cdot 9H_2O$), was obtained from Wako Chemical Co.

2.3. Fabrication of CNFs coated with PPy

The schematic diagram of the VDP procedure was illustrated in Fig. 2. A reactor for the VDP by connecting two flasks. The total volume of the reactor was about 100 mL. CNFs (0.1 g) were soaked in an initiator solution (0.1 g $FeCl_3$ in 1 mL water). After thoroughly wetting the CNFs, they were dried and moved into one chamber of the reactor equipped with a sealing apparatus. The reactor was evacuated at room temperature, and the vacuum

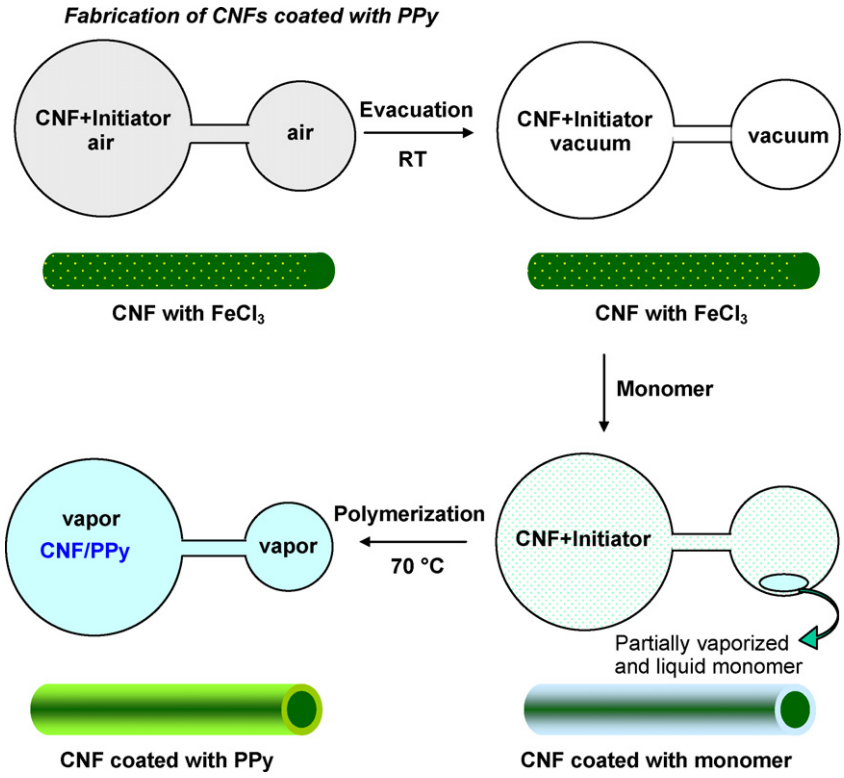

Fig. 2. Schematic procedure of the one-step VDP for fabricating PPy-coated CNFs [23].

valve was closed to obtain a static vacuum (0.1 Torr) inside the chamber. Subsequently, liquid pyrrole (Py, 0.05–0.3 mL) was introduced into the other chamber of the reactor. The Py was completely vaporized with heating at 70 °C. The VDP proceeded for 24 h at 70 °C in an atmosphere of the vaporized monomer. After polymerization, the residual monomer vapor was removed from the reactor by venting. A control experiment was performed with 0.1 g CNF, 0.2 mL Py monomer, and 0.1 g $FeCl_3$ in a 1 mL water solution as an initiator at 70 °C under 0.1 Torr for 24 h.

2.4. Characterization

Diffused reflected infrared (DRIFT) spectra were recorded on a Bomem MB 100 spectrometer at a resolution of 4 cm^{-1} with 128 scans. Images of transmission electron microscopy (TEM) were taken with JEOL JEM-200CX at an acceleration voltage of 200 kV, and the samples diluted in ethanol were cast onto a copper grid. Photographs of SEM were obtained with JEOL 6700. A microarray consisting of a pair of gold interdigitated electrodes with 80 fingers (dimensions: 10 μm spacing, 4 mm length, 50 nm thickness) was patterned on a glass substrate through photolithography [41]. Fig. 3 illustrates the side view of a sensor substrate consisting of the microelectrodes and CNF/PPy coaxial nanocables. An ethanol solution (0.1 mL) containing 10 wt.% of PPy-coated CNFs was dropped onto the substrate. Then, the PPy-coated CNFs were deposited by spin coating on the substrate for 30 s at 3000 rpm. The substrate was allowed to dry in a vacuum oven to evaporate the residual solvent. The resistance changes of the PPy-coated CNFs were measured at room temperature with a Keithley 2400 sourcemeter connected to a computer. The sensor substrate was placed in a 300 mL vacuum chamber with a vapor inlet/outlet maintained at ~1 Torr and 0.01 mL of ammonia (NH_3) or hydrochloric acid (HCl) was injected into the chamber. The concentration range of NH_3 and HCl was 10–50 ppm. The resistance was recorded in real-time at a constant current of 0.01 mA for 30 min. To verify the reversibility and reproducibility of the PPy-coated CNF sensors, the NH_3 or HCl vapor was replaced by compressed air after 1 min-exposure to the analyte vapors. The electrical conductivity was measured by a standard four-probe method under ambient conditions [42].

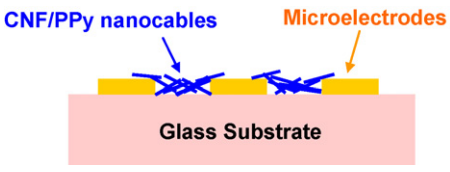

Fig. 3. Schematic illustration of a CNF/PPy coaxial nanocable sensor substrate.

3. Results and discussion

The DRIFT spectra of pristine CNFs and PPy-coated CNFs (22 nm-thickness PPy layer prepared with 0.15 mL Py monomer) are displayed in Fig. 4. The slanted baselines in the spectra of CNFs and PPy-coated CNFs were ascribed to the plasma reflection phenomenon. The absence of functional groups such as hydroxyl and carbonyl groups in the pristine CNFs was obvious from the IR spectrum in Fig. 4(a). A characteristic peak of CNFs associated with C–C–C symmetric stretching was observed at around 850 cm^{-1}. On the other hand,

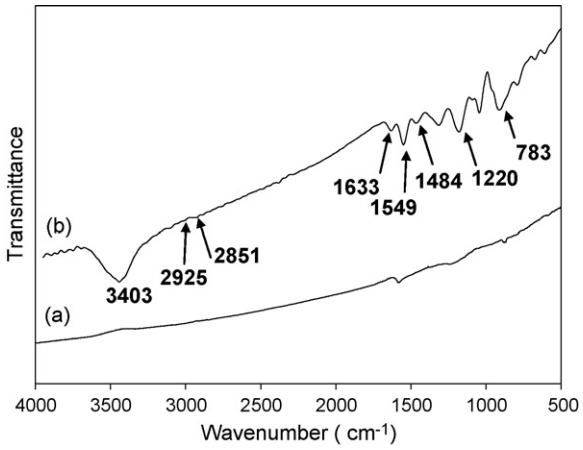

Fig. 4. DRIFT spectra of (a) pristine CNFs and (b) PPy-coated CNFs (22 nm-thickness PPy layer) prepared with 0.1 g CNF, 0.2 mL Py monomer, and 0.1 g $FeCl_3$ in 1 mL water as an initiator at 70 °C under 0.1 Torr for 24 h.

the FT-IR spectrum in Fig. 4(b) exhibited five-membered PPy ring-stretching and conjugated C–N stretching vibration bands at 1549 and 1484 cm^{-1}, respectively. C–H wagging and in-plane vibration were observed at 783 and 1220 cm^{-1}. In addition, the peaks at 2925 and 2851 cm^{-1} were associated with five-membered ring C–H stretching. The stretching and bending motion of N–H in PPy appeared at 3403 and 1633 cm^{-1}, respectively. These spectral features mean that the PPy layer was successfully introduced on the CNF surface.

Fig. 5 presents the SEM and TEM images of CNF/PPy coaxial nanocables prepared with 0.15 mL of Py monomer. The images show that the PPy-coated CNFs have uniform and thin PPy layers on the CNF surface. The formation of uniform PPy layers resulted from the characteristics of VDP and the considerably high surface area of CNF, where most of the monomers can adsorb from the vapor phase to the CNF surface. The polymerization of vaporized monomers started exclusively from the surface of CNFs owing to the adsorbed initiators and grew upward. Under these conditions, the overall polymerization was not significantly affected by polymerization in the vapor phase. Although the CNFs have a small surface roughness, the polymer layers are uniform regardless of the thickness. Judging from the FT-IR spectra and TEM images, it was evident that the one-step VDP method was successfully applied to the homogeneous coating of PPy layers onto the CNF surface with high aspect ratios.

Table 2
Variation in thickness of the deposited PPy layer as a function of the feeding amount of Py monomer

Monomer (mL)	Thickness (nm)
0.05	8 ± 1
0.10	16 ± 2
0.15	22 ± 2
0.20	26 ± 3
0.30	28 ± 3

In general, the thickness of the polymer layer was affected by the feeding amount of the Py monomer, polymerization temperature, and vacuum pressure. The most important factor affecting the thickness of the polymer layer was the monomer/substrate (CNF) (v/w) ratio and vacuum pressure inside the reaction chamber. The monomer/CNF (v/w) ratio can be tuned conveniently by adjusting the feeding amount of monomer, and the vacuum pressure was fixed at 0.1 Torr. Under these experimental conditions, the monomer/CNF (v/w) ratio was intimately proportional to the vapor pressure of feeding monomer. The variation of thickness of the PPy layer as a function of feeding amount of monomer is illustrated in Table 2. The thickness of the polymer layer tended to increase quickly below 0.15 mL, whereas increased slowly above 0.15 mL. On the other hand, the polymerization of vaporized monomers started exclusively from the surface due to the adsorbed initiators and grew upward. As the polymer layer became thicker, the residual concentration of vaporized monomers decreased and the polymer layer stopped growing at a certain point, which was denoted as a growth limit thickness. Above this point, the polymer layer cannot grow and only physical adsorption–desorption occurs on the surface of the polymer layer.

It was expected that the PPy-coated CNFs had an enhanced sensitivity owing to the synergistic combination of advantages of PPy and CNFs compared with pristine CNFs or PPy. The surface area of PPy-coated CNFs is about three times greater than

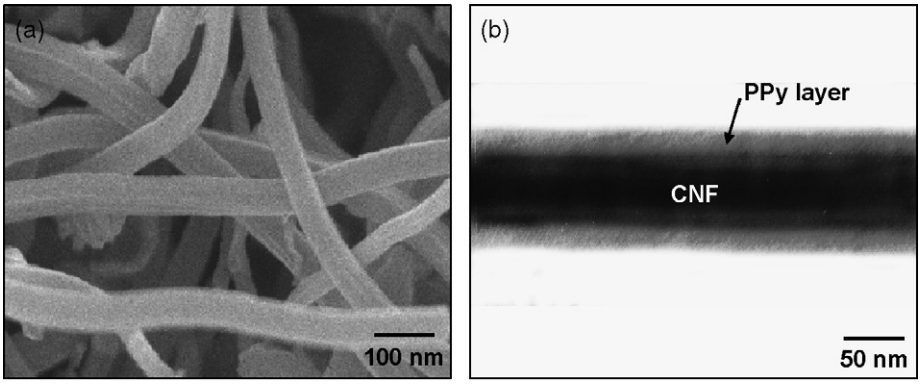

Fig. 5. (a) SEM and (b) TEM images of PPy-coated CNF (22-nm thickness PPy layer) fabricated with 0.1 g CNF, 0.2 mL Py monomer, and 0.1 g $FeCl_3$ in 1 mL of water as an initiator at 70 °C under 0.1 Torr for 24 h.

that of pristine PPy, which provides more active sites of PPy for gas adsorption [27]. Moreover, homogeneous and uniform conducting polymer layers can suppress the noises generated from structural defects [23]. The electrical conductivity of PPy-coated CNFs (22-nm thickness PPy layer) was measured to be 30 S/cm, and this was much higher than that of pristine CNFs (5 S/cm). Because the PPy layer on the one-dimensional nanofibers has a longer conjugation length compared with its bulk counterpart, the charge transport in the PPy-coated CNFs was facilitated [43,44].

The sensing mechanism of CNF/PPy nanocables is associated with the oxidation level of the PPy layer. PPy is generally a p-type semiconductor in conducting state. When appropriate counterions (anions) were introduced into the neutral PPy, the PPy backbone becomes positively charged for charge compensation. Such a doping process gives rise to the formation of charge carrier bands (polaronic/bipolaronic bands) between the interbands (valence/conduction bands) of PPy. First, the presence of polarons in the PPy chains introduces two localized electronic levels in the bandgap: bonding and antibonding cation levels. Furthermore, at higher oxidation levels, the polarons begin to interact with each other with respect to the intrachain pairing of their spins, which in turn generates the doubly charged spinless bipolarons. Importantly, the oxidation level of PPy can be readily affected by various chemical/biological species and electromagnetic waves, which may induce a change in conductance of PPy.

Fig. 6 illustrates the response signal of CNF/PPy nanocables and PPy bulks as a function of analyte concentration. The normalized resistance change is defined as $\Delta R/R_0 = (R - R_0)/R_0$, where R is the measured real-time resistance and R_0 is the initial resistance. The normalized resistance change values increased to $\Delta R/R_0 = 1$–3.5 when the concentration of NH_3 vapor increased. The detection limit (10 ppm) is comparable to the single-walled CNT/poly(*m*-aminobenzene sulfonic acid) sensors [34]. On the contrary, the absolute resistance changes dropped significantly to $\Delta R/R_0 = 0.3$–2 after addition of HCl vapor, depending on the concentration of HCl vapor. The response of CNF/PPy nanocables was proportional to the concentration of NH_3 and HCl vapors. In addition, it was remarkable that the response of CNF/PPy nanocables was extremely higher than that of the PPy bulk.

To further evaluate the sensor performance of the CNF/PPy nanocables, the sensor substrates were exposed to NH_3 (20 ppm) and HCl (20 ppm) vapors (Fig. 7). When the CNF/PPy nanocables interacted with NH_3 vapor, a dedoping reaction rapidly occurred. In other words, the introduction of NH_3 molecules into the polymer chains increased the fraction of neutral polymer chains through electron-donating to the oxidized (positively charged) polymer chains, and thus decreased the electrical conductivity due to the decrement in charge carrier density. On the other hand, the PPy chains were oxidized after exposure to HCl vapor because negatively charged chloride ions were incorporated into the PPy layer. In this case, the electrical conductivity of PPy-coated CNFs increased from procuring the polaron/bipolaron states [41]. It was noteworthy that the resistance of PPy-coated CNFs recovered close to the original level when the interaction with vapor was terminated. The response of PPy/CNF nanocables to HCl was smaller than that for NH_3, because PPy was in a doped state. Furthermore, the PPy/CNF exhibited a longer recovery time after interaction with NH_3 than HCl. These phenomena substantiated that the dedoping reaction associated with exposure to ammonia showed a higher reaction potential and a shorter reaction time than interaction with

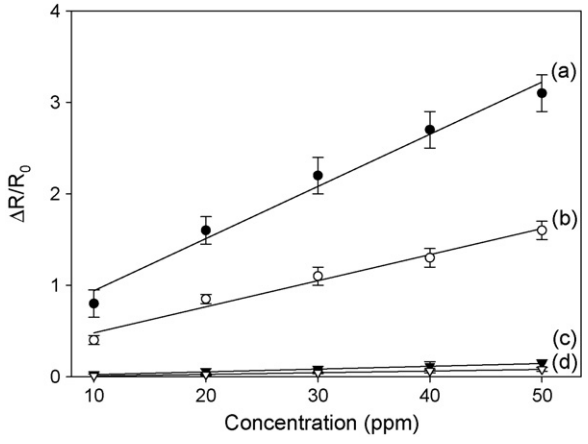

Fig. 6. Response signals (absolute values) of (a and b) CNF/PPy nanocables and (c and d) PPy bulk as a function of analyte concentration: (a and c) NH_3 and (b and d) HCl.

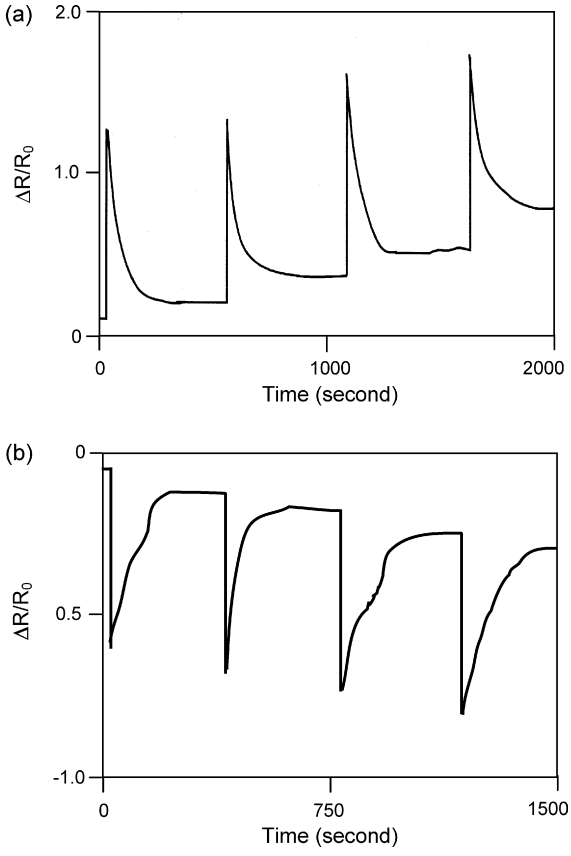

Fig. 7. Response transients of CNF/PPy nanocables (22 nm-thickness PPy layer) on periodical exposure to (a) NH_3 (20 ppm) and (b) HCl (20 ppm) vapors.

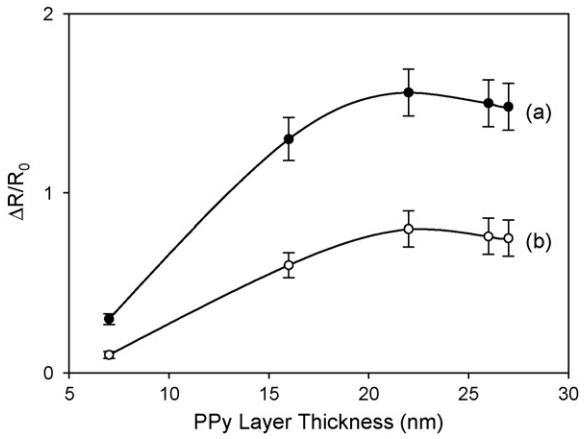

Fig. 8. Variation in normalized resistance change (absolute value) of the CNF/PPy nanocable sensors after exposure to (a) NH_3 (20 ppm) and (b) HCl (20 ppm) vapors as a function of the PPy layer thickness.

HCl. This type of test was performed more than 10 times, which demonstrated the reversibility and reproducibility of the PPy-coated CNF sensors.

On the other side, the resistance change (response signal) of CNF/PPy is inversely proportional to the contact resistance between CNF and PPy, because a high contact resistance elevates the overall resistance of CNF/PPy nanocables [27]. The enhanced response of CNF/PPy indicated that the contact resistance was relatively small compared with the initial resistance of CNF/PPy nanocables, since the homogeneous PPy layer decreased structural defects. Such a structural advantage also provided increased doping/dedoping sites, leading to enhanced response signals to both NH_3 and HCl. These facts confirmed the practicability of the VDP method for uniform coating of polymer layers. Considering the behavior of CNF/PPy coaxial nanocables, it was noteworthy that the response was quick, reversible, reproducible, and highly sensitive.

Fig. 8 illustrates the variation in normalized resistance change of PPy-coated CNFs after interaction with NH_3 and HCl as a function of the PPy layer thickness. It was revealed that the resistance change of the PPy-coated CNFs was negligible when the thickness of the PPy layer was smaller than 10 nm (a feeding amount of 0.05 mL). This is because the response of PPy-coated CNFs was dominantly affected by the inherent resistance of CNFs, showing relatively smaller resistance changes by interaction with NH_3 or HCl vapor due to the electrical neutrality of CNFs. It was remarkable that the sensitivity of PPy-coated CNFs increased significantly with increasing the PPy thickness and then stopped increasing when the PPy layer thickness was larger than the growth limit thickness point (22 nm for PPy). The adsorption–desorption motions of physically adsorbed molecules caused the signal noises above the growth limit thickness. This plateau pattern was observed in the case of interaction with both NH_3 and HCl vapors.

4. Conclusions

We demonstrated that the CNF/PPy coaxial nanocables were prepared by a simple one-step VDP method. This simple process allowed the formation of ultrathin and uniform PPy layers on the CNF surface. The thickness of the polymer layer was dependent on the loaded amount of the monomer. The CNF/PPy coaxial nanocables could be successfully employed as a highly sensitive toxic gas sensor whose response magnitude increased with increasing the NH_3 and HCl vapor concentration. The responses of the PPy-coated CNFs after interaction with NH_3 and HCl were reversible and reproducible. The responses of PPy-coated CNF sensors to NH_3 and HCl vapors were dependent on the thickness of the PPy layer on CNFs. This study is the first experimental demonstration for the realization of an elegant toxic gas sensor based on CNFs.

Acknowledgements

This work was supported by the Brain-Korea 21 Program of the Korea Ministry of Education and Korea Science and Engineering Foundation through Hyperstructured Organic Materials Research Center in Seoul National University.

References

[1] H.Y. Wang, R.T.K. Baker, Decomposition of methane to produce hydrogen and carbon nanofibers, J. Phys. Chem. B 108 (2004) 20273–20277.
[2] S. Lim, S.H. Yoon, I. Mochida, J.H. Chi, Surface modification of carbon nanofiber with high degree of graphitization, J. Phys. Chem. B 108 (2004) 1533–1536.
[3] J. Jang, J. Bae, S.-H. Yoon, A study on the effect of surface treatment of carbon nanotubes for liquid crystalline epoxide-carbon nanotube composites, J. Mater. Chem. 13 (2003) 676–681.
[4] H.W. Zhu, X.S. Li, L.J. Ci, C.L. Xu, D.H. Wu, Z.Q. Mao, Hydrogen storage in heat-treated carbon nanofibers prepared by the vertical floating catalyst method, Mater. Chem. Phys. 78 (2003) 670–675.
[5] H. Cui, S.V. Kalinin, X. Yang, D.H. Lowndes, Growth of carbon nanofibers on tipless cantilevers for high resolution topography and magnetic force imaging, Nanoletters 4 (2004) 2157–2161.
[6] M. Endo, Y.A. Kim, M. Ezaka, K. Osada, T. Yanagisawa, T. Hayashi, M. Terrones, M.S. Dresselhaus, Selective and efficient impregnation of metal nanoparticles on cup-stacked-type carbon nanofibers, Nanoletters 3 (2003) 723–727.
[7] A. Yokoyama, Y. Sato, Y. Nodasaka, S. Yamamoto, T. Kawasaki, M. Shindoh, T. Kohgo, T. Akasaka, M. Uo, F. Watari, K. Tohji, Biological behavior of hat-stacked carbon nanofibers in the subcutaneous tissue in rats, Nanoletters 5 (2005) 157–160.
[8] E. Hammel, X. Tang, M. Trampert, T. Schmitt, K. Mauthner, A. Eder, P. Potschke, Carbon nanofibers for composite applications, Carbon 42 (2004) 1153–1158.
[9] H.J. Li, J.J. Li, C.Z. Gu, Local field emission from individual vertical carbon nanofibers grown on tungsten filament, Carbon 43 (2005) 849–853.
[10] C. Singh, T. Quested, C.B. Boothroyd, P. Thomas, I.A. Kinloch, A.I. Abou-Kandil, A.H. Windle, Synthesis and characterization of carbon nanofibers produced by the floating catalyst method, J. Phys. Chem. B 106 (2002) 10915–10922.
[11] M.A. Murphy, G.D. Wilcox, R.H. Dahm, F. Marken, Adsorption and redox processes at carbon nanofiber electrodes grown onto a ceramic fiber backbone, Electrochem. Commun. 5 (2003) 51–55.
[12] A.J. Heeger, Semiconducting and metallic polymers, Angew. Chem. Int. Ed. 40 (2001) 2591–2611.
[13] J. Jang, J.H. Oh, G.D. Stucky, Fabrication of ultrafine conducting polymer and graphite nanoparticles, Angew. Chem. Int. Ed. 41 (2002) 4016–4019.
[14] J. Jang, J.H. Oh, A facile synthesis of polypyrrole nanotubes using a template-mediated vapor deposition polymerization and the conversion to carbon nanotubes, Chem. Commun. (2004) 882–883.

[15] D.T. McQude, A.E. Pullen, T.M. Swager, Conjugated polymer-based chemical sensors, Chem. Rev. 100 (2000) 2537–2574.
[16] D.B. Cairns, M.A. Khan, C. Perruchot, A. Riede, S.P. Armes, Synthesis and characterization of polypyrrole-coated poly(alkyl methacrylate) latex particles, Chem. Mater. 15 (2003) 233–239.
[17] Q. Ameer, S.B. Adeloju, Polypyrrole-based electronic noses for environmental and industrial analysis, Sens. Actuators B 106 (2005) 541–552.
[18] B.J. Tongol, C.A. Binag, F.B. Sevilla, Surface and electrochemical studies of a carbon dioxide probe based on conducting polypyrrole, Sens. Actuators B 93 (2003) 187–196.
[19] J.H. Cho, J.B. Yu, J.S. Kim, S.O. Sohn, D.D. Lee, J.S. Huh, Sensing behaviors of polypyrrole sensor under humidity condition, Sens. Actuators B 108 (2005) 389–392.
[20] G.M. Spinks, B. Xi, V.T. Truong, G.G. Wallace, Actuation behaviour of layered composites of polyaniline, carbon nanotubes and polypyrrole, Synth. Met. 151 (2005) 85–91.
[21] L. Ruangchuay, A. Sirivat, J. Schwank, Selective conductivity response of polypyrrole-based sensor on flammable chemicals, React. Funct. Polym. 61 (2004) 11–22.
[22] J.M. Charlesworth, A.C. Partridge, N. Garrard, Interaction between poly(pyrrole) and organic vapors, J. Phys. Chem. 97 (1993) 5418.
[23] J. Jang, B. Lim, Facile fabrication of inorganic-polymer core-shell nanostructures by a vapor deposition polymerization, Angew. Chem. Int. Ed. 42 (2003) 5600–5603.
[24] J. Jang, B. Lim, J. Lee, T. Hyeon, Fabrication of a novel polypyrrole/poly(methyl methacrylate) coaxial nanocable using mesoporous silica as a nanoreactor, Chem. Commun. (2001) 83–84.
[25] M. Penza, E. Milella, V.I. Anisimkin, Monitoring of NH3 gas by LB polypyrrole-based SAW sensor, Sens. Actuators B 47 (1998) 218–224.
[26] J. Travas-Sejdic, H. Peng, P.A. Kilmaitin, M.B. Cannell, G.A. Bowmaker, R.P. Cooney, C. Soeller, DNA sensor based on functionalized polypyrrole, Synth. Met. 152 (2005) 37–40.
[27] K.H. An, S.Y. Jeong, H.R. Hwang, Y.H. Lee, Enhanced sensitivity of a gas sensor incorporating single-walled carbon nanotube-polypyrrole nanocomposites, Adv. Mater. 16 (2004) 1005–1009.
[28] L.H. Dall'Antonia, M.E. Vidotti, S.I.C. de Torresi, R.M. Torresi, A new sensor for ammonia determination based on polypyrrole films doped with dodecylbenzenesulfonate (DBSA) ions, Electroanalysis 14 (2002) 1577–1586.
[29] N. Guernion, R.J. Ewen, K. Pihlainen, N.M. Ratcliffe, G.C. Teare, A highly sensitive polypyrrole sensor and its electrical responses to amines of differing basicity at high humidities, Synth. Met. 126 (2002) 301–310.
[30] I. Lahdesmaki, W.W. Kubiak, A. Lewenstam, A. Ivaska, Interferences in a polypyrrole-based amperometric ammonia sensor, Talanta 52 (2000) 269–275.
[31] A.V. Samoylov, V.M. Mirsky, Q. Hao, C. Swart, Y.M. Shirshov, O.S. Wolfbeis, Nanometer-thick SPR sensor for gaseous HCl, Sens. Actuators B 106 (2005) 369–372.
[32] S. Virji, J. Huang, R.B. Kaner, B.H. Weiller, Polyaniline nanofiber gas sensors: examination of response mechanisms, Nanoletters 4 (2004) 491–495.
[33] J. Suehiro, G.B. Zhou, M. Hara, A carbon nanotube-based gas sensor using dielectrophoresis and its application for ammonia detection, J. Phys. D Appl. Phys. 36 (2003) L109–L114.
[34] E. Bekyarova, M. Davis, T. Burch, M.E. Itkis, B. Zhao, S. Sunshine, R.C. Haddon, Chemically functionalized single-walled carbon nanotubes as ammonia sensors, J. Phys. Chem. B 108 (2004) 19717–19720.
[35] O.K. Varghese, P.D. Kichambre, D. Gong, K.G. Ong, E.C. Dickey, C.A. Grimes, Gas sensing characteristics of multi-wall carbon nanotubes, Sens. Actuators B: Chem. 81 (2001) 32–41.
[36] V. Bavastrello, E. Stura, S. Carrara, V. Erokhin, C. Nicolini, Poly(2,5-dimethylaniline)-MWNTs nanocomposite: a new material for conductometric acid vapours sensor, Sens. Actuators B 98 (2004) 247–253.
[37] S. Chopra, A. Pham, J. Gaillard, A. Parker, A.M. Rao, Carbon-nanotube-based resonant-circuit sensor for ammonia, Appl. Phys. Lett. 80 (2002) 4632–4634.
[38] J. Jang, H. Yoon, Multigram-scale fabrication of monodisperse conducting polymer and magnetic carbon nanoparticles, Small 1 (2005) 1195–1199.
[39] J. Jang, Y. Nam, H. Yoon, Fabrication of polypyrrole-poly(*N*-vinylcarbazole) core-shell nanoparticles with excellent electrical and optical properties, Adv. Mater. 17 (2005) 1382–1386.
[40] R.J. Best, W.W. Russell, Nickel, copper and some of their alloys as catalysts for ethylene hydrogenation, J. Am. Chem. Soc. 76 (1954) 838.
[41] J. Jang, M. Chang, H. Yoon, Chemical sensors based on highly conductive PEDOT nanorods, Adv. Mater. 17 (2005) 1616–1620.
[42] I.A. Belous, O.V. Utas, D.A. Tsukanov, V.G. Lifshitz, In situ conductance measurement of surface phases on silicon by the four-probe method, Instrum. Exp. Tech. 44 (2001) 698–704.
[43] J. Jang, H. Yoon, Facile fabrication of polypyrrole nanotubes using reverse microemulsion polymerization, Chem. Commun. (2003) 720–721.
[44] J. Jang, H. Yoon, Formation mechanism of conducting polypyrrole nanotubes in reverse micelle systems, Langmuir 21 (2005) 11484–11489.

Biographies

Jyongsik Jang received PhD degree from Case Western Reserve University (Cleveland, USA) in 1988. Then he joined as a faculty member in the School of Chemical and Biological Engineering at Seoul National University (Korea) in 1991. His research background focused on the adhesion promotion of polymer composite interface. Since 2000, numerous remarkable researches on fabrication of polymer nanomaterials and their applications have been conducted in his research group.

Joonwon Bae obtained PhD degree from Seoul National University (Korea) in August 2005. Then he joined as a post-doctoral research fellow in the Professor Thomas P. Russell research group at University of Massachusetts Amherst (USA) in October 2005. He has been interested in the fabrication and applications of polymer and carbon nanostructures. Currently, he studies on the electrohydrodynamic instability of homopolymer or copolymer thin films.